Annealed Samples of Some Tetrafluoroethylene Perfluorinated Copolymers Studied by Small- and Wide-Angle X-ray Scattering and Differential Scanning Calorimetry

Antonio Marigo,* Carla Marega, and Roberto Zannetti

Dipartimento di Chimica Inorganica, Metallorganica ed Analitica dell'Universitá, via Loredan 4, I-35131 Padova, Italy

Giuseppe Ajroldi and Anna Staccione

AUSIMONT S.p.A. Bollate (Milano), Italy

Received February 25, 1997; Revised Manuscript Received July 8, 1997[⊗]

ABSTRACT: Some quenched and annealed samples of tetrafluoroethylene copolymers containing perfluoropropyl vinyl ether, perfluoromethyl vinyl ether, and hexafluoropropene were studied by small-angle X-ray scattering and differential scanning calorimetry. Small-angle X-ray scattering experimental spectra were analyzed by a fitting method with the profiles calculated from some theoretical distribution models of the lamellar thickness. The mathematical evaluation of small-angle X-ray scattering patterns has provided crystallinity values which were compared with those obtained by wide-angle X-ray scattering in order to obtain information on the organization of the lamellar stacks. The experimental results allow one to conclude that, during the annealing of the quenched fluorinated copolymers, at increasing temperatures, the melting of the thin lamellae takes place together with the appearance and the growth of nonlamellar crystallites.

Introduction

In a previous paper[1] we described an investigation on lamellar-shaped superstructures observed in some random copolymers of tetrafluoroethylene (TFE) containing as comonomers perfluoropropyl vinyl ether, CF_3-$CF_2CF_2OCF{=}CF_2$ (FPVE), perfluoromethyl vinyl ether, $CF_3OCF{=}CF_2$ (FMVE), and hexafluoropropene (HFP). The investigation was mostly carried out by small-angle X-ray scattering (SAXS), a technique which allows the measurement of the lamellar and amorphous layer thicknesses by studying the monodimensional correlation functions. Furthermore, the percent of crystallinity and the unit cell parameters were determined, by wide-angle X-ray scattering (WAXS) measurements. The results obtained allowed one to conclude that a partial inclusion of the CF_3 groups in the PTFE crystalline unit cell takes place, while the $O(CF_2)_2CF_3$ groups are arranged in the amorphous regions.

The morphological features and structural parameters of these copolymers depend strongly on the kind and concentration of the comonomer: in parallel, the physicochemical properties seem to be closely related to the microstructural ones; moreover, such properties are modified by both the processing treatments and the utilization conditions. In consequence, a structural investigation can be useful for copolymer samples prepared under different crystallization conditions and successive annealing treatments. The present paper describes an analysis of the copolymer samples TFE−FPVE (PFA), TFE−FPVE−FMVE (MFA), and TFE−HFP (FEP), quenched from the melt and annealed at different temperatures. The selected experimental techniques were SAXS, WAXS, and differential scanning calorimetry (DSC); some density measurements were also carried out. In particular, by SAXS, it was possible to make an evaluation not only of the average thicknesses of the crystalline and amorphous regions but also of the thickness distribution, which was evaluated by comparing the patterns calculated from some theoretical distribution models and the experimental patterns.[2]

Table 1. Comonomer Content and Melt Flow Index (MFI) of the Examined Samples

sample	comonomer	mole % of comonomer	MFI[a] (g/10′)
PFA	FPVE	1.7	2.9
MFA	FPVE−FMVE	3.9	3.2
FEP	HFP	6.7	2.9

[a] Determined at 372 °C/5 kg.

Experimental Section

Samples. The examined copolymers were prepared by emulsion polymerization in the laboratories of AUSIMONT S.p.A., Bollate (Milano). The kind and the percent of comonomer and the corresponding melt flow index (MFI) data are reported in Table 1. The MFI data were considered to be inversely related to the molecular weight, since the insolubility of these copolymers prevents an alternative determination of the molecular weights. Samples which are successively indicated as /A were prepared by compression molding granules and quenching from the melt down to room temperature, according to the ASTM D 3307−86 procedure. The samples indicated as /C1, /C2, and /C3 were obtained by annealing for 20 h, in a circulating air oven, the /A samples at T_a temperatures of 40, 20 and 10 °C lower than the melting temperatures of the /A samples, determined by DSC measurements.

The DSC analysis was carried out with a PERKIN ELMER DSC7 instrument, following the ASTM D 3417 and D 3418 procedures, at a scanning rate of 10 °C/min. The density values were determined on /A to /C3 samples by measuring the weight of a sample in air and then immersed in water, according to the ASTM D 792 method. Table 2 reports the crystallization conditions and the densities of the specimens.

Wide-Angle X-ray Scattering. WAXS patterns were recorded with a SEIFERT MZ III powder diffractometer, equipped with a graphite monochromator on the diffracted beam, in the angular range $2\theta = 5-50°$, with steps of 0.1° (2θ) and 10 s of recording time for each step. Cu Kα X-radiation was employed.

* Phone: +39-49-8275154. E-mail: marigo@uxl.unipd.it.

[⊗] Abstract published in *Advance ACS Abstracts,* November 15, 1997.

S0024-9297(97)00254-4 CCC: $14.00

Table 2. Crystallization Condition and Density (*d*) of the Examined Samples

sample	crystallization condition	d (g/cm^3)
PFA/A	quenched (ASTM D 3307−86)	2.1323
PFA/C1	annealed at 265 °C	2.1494
PFA/C2	annealed at 285 °C	2.1562
PFA/C3	annealed at 295 °C	2.1588
MFA/A	quenched (ASTM D 3307−86)	2.1269
MFA/C1	annealed at 250 °C	2.1398
MFA/C2	annealed at 270 °C	2.1456
MFA/C3	annealed at 280 °C	2.1443
FEP/A	quenched (ASTM D 3307−86)	2.1396
FEP/C1	annealed at 222 °C	2.1535
FEP/C2	annealed at 242 °C	2.1524
FEP/C3	annealed at 252 °C	2.1500

By applying the least-squares fitting procedure elaborated by Hindeleh and Johnson,[3] an evaluation was possible of the degree of crystallinity (wt %) of the specimens, successively transformed in volume-crystallinity Φ_{WAXS} by the density values of the amorphous and crystalline phases, reported in the literature.[4,5] The relative error was estimated as 1% for Φ_{WAXS}, by repeating the fitting procedure for different statistical weights and experimental values.

Small-Angle X-ray Scattering. SAXS patterns were recorded with a Kratky camera, using Cu Kα X-radiation. The intensity data were collected with a MBraun OED-50M position-sensitive detector in the angular range 0.1−5.0° (2θ) and were successively corrected for the blank scattering. A constant continuous background scattering was then subtracted,[6] and the obtained intensity values $\tilde{I}(s)$ were smoothed in the tail region, with the aid of the $s\tilde{I}(s)$ vs $1/s^2$ plot.[7]

The thickness of the transition layer E between the lamellar and the amorphous regions was evaluated according to the procedure described by Vonk:[7] the standard deviation of the E values is 20%, estimated by applying different fitting ranges in the linear region of the $s\tilde{I}(s)$ vs $1/s^2$ plot. The scattering functions $\tilde{I}(s)$ were then multiplicated for the factor[8] $(1 - 2\pi^2E^2s^2/3)^{-1}$, in order to correct them for the transition layer (E). Finally, the Vonk's desmearing procedure[9] was applied and the one-dimensional scattering function was obtained by the Lorentz correction $I_1(s) = 4\pi s^2 I(s)$, where $I_1(s)$ is the one-dimensional scattering function and $I(s)$ the desmeared intensity function, with $s = (2/\lambda) \sin \theta$.

Theoretical Evaluation of the SAXS Patterns. The evaluation of the SAXS patterns according to some theoretical distribution models[2,8] was carried out referring to the Hosemann model,[10] which assumes the presence of lamellar stacks having an infinite side dimension. This assumption, in practice, takes into account a monodimensional electron density change along the direction normal to the lamellae. According to this model, the intensity profile is evaluated as

$$I(s) = I'(s) + I''(s) \tag{1}$$

where

$$I'(s) = \frac{(\rho_c - \rho_a)^2}{4\pi^2 s^2 D} \frac{|1 - F_C|^2(1 - |F_A|^2) + |1 - F_A|^2(1 - |F_C|^2)}{|1 - F_C F_A|^2} \tag{2}$$

$$I''(s) = \frac{(\rho_c - \rho_a)^2}{2\pi^2 s^2 DN} \mathrm{Re}\left\{\frac{F_A(1 - F_C)^2(1 - (F_A F_C)^N)}{(1 - F_A F_C)^2}\right\} \tag{3}$$

In these equations, F_C and F_A represent the Fourier transforms of the Gaussian distribution functions of the lamellar thicknesses C and of the amorphous regions A, ρ_c and ρ_a are the electron densities of the crystalline and amorphous regions, respectively, N is the number of lamellae in the stack, and D is the average long period.

The optimized parameters were the average lamellar thickness C, the Gaussian distribution standard deviation of the lamellar thickness σ_C, $\Phi_{SAXS} = C/D$, and N, while the average thickness of the amorphous regions $A = [(1 - \Phi_{SAXS})/\Phi_{SAXS}]C$ and its Gaussian distribution standard deviation $\sigma_A = (\sigma_C/C)A$. The errors were estimated as 1% for Φ_{SAXS} and C, by repeating the fitting procedure, as described for Φ_{WAXS}. Figure 1 reports, as an example, the fit obtained for the PFA/C1 sample.

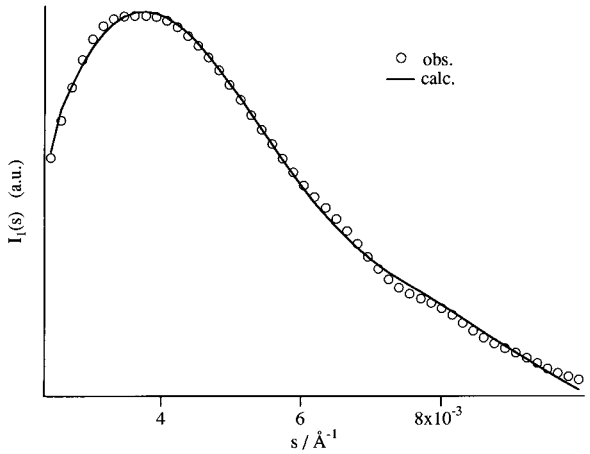

Figure 1. Best fit between experimental and calculated small-angle one-dimensional scattering functions of the PFA/C1 sample.

Table 3. Crystallinity by Small- (Φ_{SAXS}) and Wide-Angle (Φ_{WAXS}) X-ray Scattering Measurements

sample	Φ_{WAXS}	Φ_{SAXS}
PFA/A	0.39	0.39
PFA/C1	0.46	0.37
PFA/C2	0.47	0.31
PFA/C3	0.50	0.30
MFA/A	0.36	0.34
MFA/C1	0.41	0.35
MFA/C2	0.45	0.32
MFA/C3	0.46	0.31
FEP/A	0.37	0.33
FEP/C1	0.43	0.35
FEP/C2	0.41	0.30
FEP/C3	0.40	0.31

Results and Discussion

The crystallinity values Φ_{WAXS} and Φ_{SAXS} for all the examined samples are reported in Table 3.

By considering the Φ_{WAXS} data, an increase of crystallinity can be noted from the /A samples to the corresponding annealed ones; furthermore, while in PFA and MFA the crystallinity increases with the annealing temperature, in FEP it slightly decreases, and this observation is confirmed by the density data reported in Table 2.

It is known that the main effect of the annealing at increasing temperatures is generally associated with an increase of the lamellar thickness, of the density, and of the melting temperature. As concerns the previously reported differences among the PFA, MFA, and FEP samples, a probable interpretation could be based on the higher comonomer percent and/or a partial insertion of the CF_3 groups in the crystalline phase.[1] However, an interpretation is difficult of the Φ_{WAXS} and density data (Tables 3 and 2), and it is necessary to consider also other information, reported below and obtained by SAXS and DSC measurements.

In Table 3 it can be noted that the crystallinity Φ_{SAXS} is the same as the corresponding Φ_{WAXS} value only for the quenched sample PFA/A, while it is slightly different for MFA/A and FEP/A. For the annealed samples, the Φ_{SAXS} values are always lower than Φ_{WAXS} and they show a decreasing trend with increasing T_a tempera-

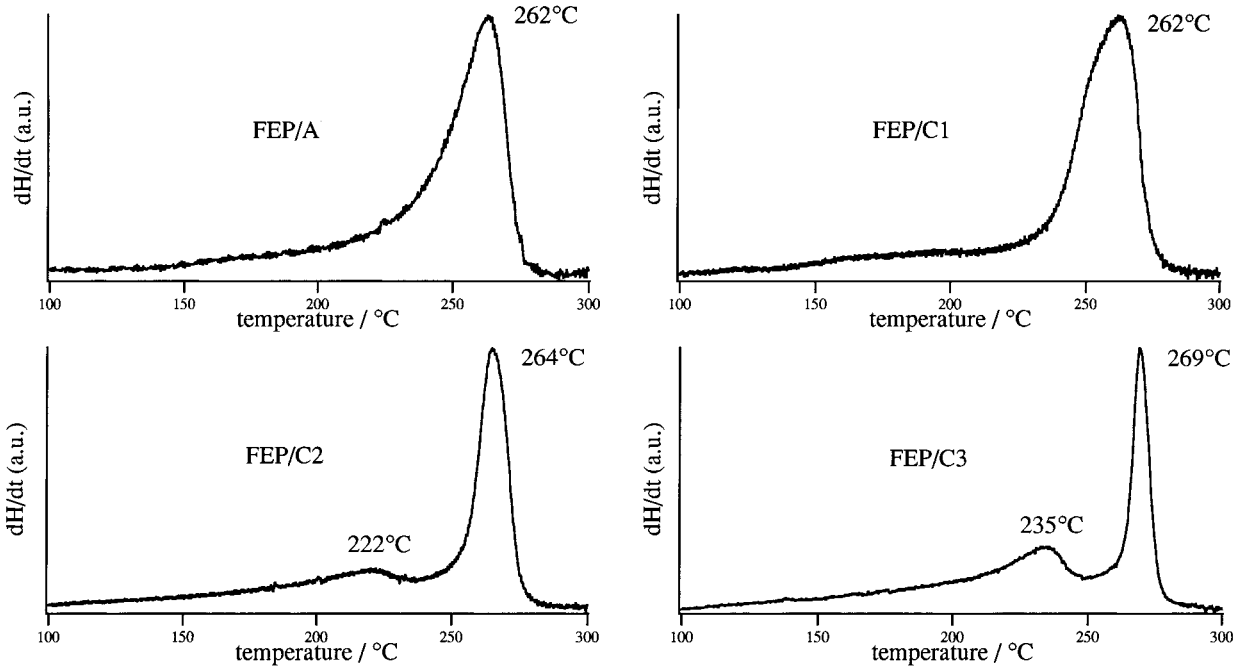

Figure 2. Differential scanning calorimetry patterns of the FEP samples.

Table 4. Average Values of the Transition Layer Thickness (*E*), the Long Period (*D*), the Lamellae and Amorphous Layer Thicknesses (*C* and *A*), and the Relative Dispersion of the Lamellar Thickness (σ_C/C)

sample	*E* (Å)	*D* (Å)	*C* (Å)	*A* (Å)	σ_C/C
PFA/A	10	163	63	100	0.41
PFA/C1	11	210	77	133	0.35
PFA/C2	11	246	80	166	0.36
PFA/C3	11	265	81	184	0.41
MFA/A	10	171	58	113	0.36
MFA/C1	10	187	66	121	0.39
MFA/C2	11	198	62	136	0.47
MFA/C3	9	202	62	140	0.45
FEP/A	12	181	60	121	0.37
FEP/C1	12	193	67	126	0.40
FEP/C2	11	205	62	143	0.40
FEP/C3	12	207	59	148	0.34

Table 5. Melting Enthalpies (ΔH_{m1}, ΔH_{m2}, $\Delta H_{m\ tot}$) and Temperatures (T_{m1}, T_{m2}) Determined by DSC

sample	T_{m1} (°C)	ΔH_{m1} (cal/g)	T_{m2} (°C)	ΔH_{m2} (cal/g)	$\Delta H_{m\ tot}$ (cal/g)
PFA/A	305	6.0			6.0
PFA/C1	305	7.8			7.8
PFA/C2	308	7.1	255	1.1	8.2
PFA/C3	310	6.4	273	2.2	8.6
MFA/A	290	5.1			5.1
MFA/C1	288	5.7			5.7
MFA/C2	289	5.3	240	1.0	6.3
MFA/C3	293	4.6	255	1.5	6.1
FEP/A	262	4.7			4.7
FEP/C1	262	5.5			5.5
FEP/C2	264	4.3	222	1.8	6.1
FEP/C3	269	3.3	235	2.8	6.1

tures. It is to be noted that while the WAXS data are determined by the whole volume of the scattering sample, the SAXS crystallinity, being evaluated by the lamellar periodicity peak, only accounts for the regions which are organized in lamellar stacks. In conclusion, while the sample PFA/A seems to be completely organized in lamellar stacks, in the remaining samples more or less evident crystalline regions are detected outside the stacks, and only the WAXS technique can in some way take them into account.

Table 4 reports the average long period, the average thicknesses of the transition layer and the lamellar and amorphous regions and the relative dispersion of the lamellar thicknesses. As concerns the transition layer *E*, it can be observed that the obtained data do not seem dependent on the kind of comonomer and on the procedure of the crystallization process. The long period increases considerably, especially for PFA, if one considers the data of the samples /A to /C3, and it also can be observed that its value increases with the annealing temperature.

Only in the PFA samples does the average lamellar thickness increase considerably with T_a, while in the case of MFA and FEP it first increases for the sample annealed at the lowest temperature and then decreases with increasing T_a. It can be concluded that the rise of the long period is mainly associated with a parallel increase of the average thickness of the amorphous regions (see Table 4). An effect of the annealing could be hypothesized that produces a melting of the thinner lamellae and a consequent rise of the average value of the amorphous layers. The increase with T_a of the WAXS crystallinity, mainly detected for PFA and MFA samples, could be associated with the rise and growth of thin lamellae out of the lamellar stacks or nonlamellar microcrystals. As concerns the values of σ_C/C, rather wide distributions can be observed, but any change of the crystallization parameters does not give rise to parallel, noticeable changes of the thickness distribution.

The DSC measurements show some peculiar effects which support the X-ray scattering data. An example is shown for FEP in Figure 2, and the data obtained for all the samples are collected in Table 5. Annealing well below the melting temperature (samples/C1) brings about an increase in the melting enthalpy, and a shoulder, which merges with the main melting peak, appears on its low-temperature side. In other words the high-melting fraction is increased not only because the low-melting fraction is disappearing but also through a rearrangement of a fraction of the disordered phase.

Furthermore, the DSC data show the presence of an endothermal melting peak, having a broadened shape,

at a lower temperature than that of the main peak, for the annealed specimens of the /C2 and /C3 groups. The melting temperature corresponding to this secondary peak (T_{m2}) is always lower than the corresponding annealing temperature T_a and increases with T_a (see Table 5), while the melting temperatures T_{m1} of the main endothermal peak are practically constant from /A to /C1 and successively increase with T_a.

Such behavior is not unexpected, and several examples can be found in the literature.[11] Khanna et al.[12] demonstrated the appearance of secondary endothermal melting peaks in annealed films of ethylene−chlorotrifluoroethylene copolymers, and they supposed the rise of lower melting crystals in the amorphous fraction.

Table 5 shows that the melting enthalpy values (ΔH_{m2}), determined for the secondary peak, increase with the annealing temperature, while the ΔH_{m1} ones show a similar behavior to the Φ_{SAXS} crystallinity (taking obviously into account the relationship between crystallinity and melting enthalpy). Moreover the total melting enthalpy $\Delta H_{m\ tot} = \Delta H_{m1} + \Delta H_{m2}$ values seem to agree with the trend of the Φ_{WAXS} values.

According to the above experimental data, it can be supposed that the main melting peak could be related to the matter organized in lamellar stacks; the associated melting enthalphy is related to the melting of thin lamellae in the stacks, and is dependent on the previous annealing history. On the other side the occurrence of the secondary melting peak and the increase of its melting enthalpy ΔH_{m2} with the annealing temperature could be interpreted in terms of the rise and growth of microcrystals.

The more defective chains, i.e. the chains which probably contain larger amounts of comonomer, unable to contribute to the growth of thick and stacked lamellae, recrystallize by thin and not stacked lamellae or nonlamellar microcrystals melting at low temperature. This is well demonstrated by DSC traces measured on samples /C2 and /C3, where two populations of crystallites differing in melting points are observed, and by the above cited consideration based on Φ_{WAXS}, Φ_{SAXS}, and SAXS parameters.

Conclusions

The WAXS and SAXS techniques, joined with the DSC one, show that, during the annealing process of the examined fluorinated copolymers, a melting phenomenon takes place of thin lamellae and that, in consequence, the long-period parameters increase; at the same time, the rise takes place of thin lamellae out of the lamellar stacks or nonlamellar microcrystals, originated in the amorphous fraction. An increase of the annealing temperature produces an increase and a growth of these crystals and, in consequence, an increase of their melting point. Finally, the difference must be underlined among data obtained by the employed experimental techniques that, being strictly complementary, allowed an improvement of the morphological picture related to the annealing process.

Acknowledgment. The authors thank the MURST (Ministero per l'Università e la Ricerca Scientifica e Tecnologica) of Italy for financial support, the CUGAS (Centro Universitario Grandi Apparecchiature Scientifiche) of the University of Padova for making available the SAXS instrumentation, and AUSIMONT S.p.A. for permission to publish this paper.

References and Notes

(1) Marigo, A.; Marega, C.; Zannetti, R.; Ajroldi, G. *Macromolecules* **1996**, *29*, 2197.
(2) Marega, C.; Marigo, A.; Cingano, G.; Zannetti, R.; Paganetto, G. *Polymer* **1996**, *37*, 5549.
(3) Hindeleh, A. M.; Johnson, D. J. *J. Phys. D* **1971**, *4*, 259.
(4) Clark, E. S. *Bull. Am. Phys. Soc.* **1962**, *18*, 317.
(5) Vonk, C. G. Synthetic Polymers in the Solid State. In *Small Angle X-ray Scattering*; Glatter, O., Kratky, O., Eds.; Academic Press: London, 1982.
(6) Vonk, C. G.; Pijpers, A. P. *J. Polym. Sci., Part B: Polym. Phys.* **1985**, *23*, 2517.
(7) Vonk, C. G. *J. Appl. Crystallogr.* **1973**, *6*, 81.
(8) Blundell, D. J. *Polymer* **1978**, *18*, 1343.
(9) Vonk, C. G. *J. Appl. Crystallogr.* **1971**, *4*, 340.
(10) Hosemann, R.; Bagchi, S. N. *Direct Analysis of Diffraction by Matter*; North Holland: Amsterdam, 1962.
(11) Turi, E. A. *Thermal Characterization of Polymeric Materials*; Academic Press: Orlando, FL, 1981.
(12) Khanna, Y. P.; Turi, E. A.; Sibilia, J. P. *J. Polym. Sci., Polym. Phys. Ed.* **1984**, *22*, 2175.

MA970254D